Short Communication

Cellular senescence predicts treatment outcome in metastasized colorectal cancer

AM Haugstetter[1], C Loddenkemper[2], D Lenze[3], J Gröne[4], C Standfuß[5], I Petersen[6], B Dörken[1,7], and CA Schmitt[*,1,7]

[1]*Molekulares Krebsforschungszentrum der Charité – MKFZ, Charité - Universitätsmedizin Berlin, Germany;*

[2]*Technische Universität München, Institute of Pathology, Munich, Germany;*

[3]*Department of Pathology, Campus Benjamin Franklin, Charité - Universitätsmedizin Berlin, Germany;*

[4]*Department of General, Vessel and Thorax Surgery, Campus Benjamin Franklin, Charité - Universitätsmedizin Berlin, Germany;*

[5]*Free University, Department of Bioinformatics, Berlin, Germany;*

[6]*Friedrich Schiller University, Department of Pathology, Jena, Germany;*

[7]*Max-Delbrück-Center for Molecular Medicine, Berlin, Germany*

[*]Correspondence: Prof. Dr. Clemens A. Schmitt, Medical Department of Hematology, Oncology and Tumor Immunology, Campus Virchow Clinic, Molekulares Krebsforschungszentrum, Charité - Universitätsmedizin Berlin, and Max-Delbrück-Center for Molecular Medicine, Augustenburger Platz 1, 13353 Berlin, Germany; E-mail: clemens.schmitt@charite.de

Running title: Cancer cell senescence predicts treatment outcome

STRUCTURED ABSTRACT

BACKGROUND: Cellular senescence is a terminal cell-cycle arrest that occurs in response to activated oncogenes and DNA-damaging chemotherapy. Whether cancer cell senescence at diagnosis might be predictive for treatment outcome is unknown.

METHODS: A senescence index (SI) was developed and used to retrospectively correlate the treatment outcome of 30 UICC stage IV colorectal cancer (CRC) patients with their SI at diagnosis.

RESULTS: 5-fluorouracil/leucovorin-treated CRC patients achieved a significantly longer progression-free survival when presenting with SI-positive tumours prior to therapy (median 12.0 *vs.* 6.0 months; $P = 0.044$).

CONCLUSION: Cancer cell senescence predicts treatment outcome in metastasized CRC. Prospective analyses of larger patient cohorts are needed.

INTRODUCTION

In the past, many cancer studies sought to link quantitative assessments of tumour growth properties, namely proliferation and apoptosis, to treatment outcome, but the majority of these analyses produced negative results for various reasons. Although relevant as a prognosticator, the value of utilizing the mitotic index to predict treatment outcome is very limited (see (Brown & Attardi, 2005; Schmitt, 2003; Schmitt, 2007; Yerushalmi et al., 2010) for review and references therein). A third cancer-related growth condition is oncogene-induced senescence (OIS), a terminal cell-cycle arrest initiated by activated Ras-type oncogenes that acts as a tumour-suppressive barrier in pre-malignant lesions *in vivo* (Braig et al., 2005; Collado & Serrano, 2010; Michaloglou et al., 2005; Reimann et al., 2010). OIS is mediated *via* an oncogene-evoked DNA damage response (DDR) (Bartkova et al., 2005; Bartkova et al., 2006; Gorgoulis et al., 2005), thereby explaining why DNA-damaging chemotherapy produces senescence as well (Chang et al., 1999; Schmitt et al., 2002). Therapy-induced senescence (TIS) contributes to treatment outcome in pre-clinical models (Schmitt et al., 2002), and is detectable in patient cancer biopsies after neoadjuvant chemotherapy (Roberson et al., 2005; te Poele et al., 2002), but its long-term impact on clinical courses remains

undetermined. We hypothesized that sporadically senescent cells present in untreated cancers at diagnosis may indicate an increased susceptibility to TIS, and, thus, might be associated with a superior clinical outcome. Since the gold-standard senescence assay, detection of the senescence-associated β-galactosidase (SA-β-gal) activity (Dimri et al., 1995), cannot be applied to formalin-fixed and paraffin-embedded (FFPE) clinical routine samples, we developed a senescence index (SI) based on FFPE-suitable immunohistochemical surrogate markers. We report here the first-time utilization of this SI in untreated human tumour specimens at diagnosis as a predictor for outcome to cancer therapy.

MATERIALS AND METHODS

Patients and tumour material

Snap-frozen or formalin-fixed and paraffin-embedded (FFPE) samples of normal colon mucosa, colon adenoma and colon carcinoma were collected, and informed patient consent was obtained for the anonymous use of the material. FFPE tumour samples from previously untreated 30 patients with UICC stage IV colorectal cancer (CRC) who all received a 5-fluorouracil/leucovorin (5-FU/LV)-based first-line regimen were subjected to senescence evaluation, reflecting the available archive material in our pathology department between the years 1996 and 2003 that met these criteria. Tissue material from patients suspected or diagnosed with a hereditary cancer syndrome or inflammatory bowel disease, or whose chemotherapy was terminated for reasons other than disease progression was excluded from this study. Clinical data sets were compiled in a retrospective and anonymous manner, and included gender, age, tumour location, carcinoembryonic antigen (CEA) serum levels, TNM classification, tumour grading and progression-free survival (PFS), defined as the time from first diagnosis until diagnosis of progressive disease (*i.e.* local recurrence of the primary lesion, or growth of metastases, or occurrence of new metastatic lesions).

Retroviral infection

IMR90 human fibroblasts (CCl-186 from American Type Culture Collection, Manassas, VA, USA) were stably transduced with the pBabe-Puro-H-*Ras*V12 retrovirus (provided by S. Lowe) or an empty vector as a control, and selected in puromycin as described (Braig et al., 2005; Serrano et al., 1997). Cell pellets were snap-frozen in liquid nitrogen or processed as FFPE pellets comparable to patient tissue samples.

Immunohistochemical analysis

Cryosections (12 μm) were acetone-fixed and exposed to an anti-Ki67 primary antibody (M7240, Dako, Glostrup, Denmark, 1:250 dilution) for 30 min. Antibody binding was visualized *via* a chromogenic substrate in a streptavidin/alkaline phosphatase-amplified secondary antibody according to the manufacturer's recommendations (K0689, K0698, K0625, X3021, all from Dako).

FFPE sections (7 μm) were subjected to heat-induced antigen retrieval prior to incubation with primary antibodies for 30 minutes. Primary antibodies against Ki67 (as above), heterochromatin protein 1γ (HP1γ; MAB3450, Chemicon/Millipore, Billerica, MA, USA, 1:250), phospho-activated ERK1/2 (p-ERK; #4376, Cell Signaling Technology [CST], Danvers, MA, USA, 1:50), plasminogen activator inhibitor-1 (PAI-1 [*i.e.* Ncl-PAI-1]; Novocastra, Newcastle upon Tyne, UK, 1:20), or cleaved caspase 3/Asp175 (#9661, CST, 1:200) were used, followed by the appropriate secondary antibody plus a streptavidin/alkaline phosphatase conjugate or streptavidin/peroxidase kit and suitable chromogenic substrates such as DAB (3,3´-diaminodbenzidine) or Fast Red (K0690, K3468, K5005, all from Dako).

The formula and the cut-off values of the senescence index (SI) were generated based on the expression (*i.e.* the percentage of positive cells by immunostaining) of the three markers p-ERK, HP1γ and PAI-1 in low-proliferating areas (arbitrarily defined as < 12 Ki67-positive in an area of 100 cells) in a learning set of five adenoma samples. For each of the three markers, a factor was generated that reflects the reciprocal percentage of cells that stained positive in such areas averaged over these five adenomas. This factor was used as a coefficient to equalize the marker's relative individual contribution to the SI. Moreover, a linear correction value was added to set the discrimination threshold to 0. Values between −1 and +1 were considered "non-conclusive". SI values of individual cancer samples were obtained in low-proliferating areas as well. See Figure 2 for further information on SI-related technical procedures.

Senescence-associated β-galactosidase activity

Senescence-associated β-galactosidase (SA-β-gal) activity was detected at pH 6.0 in cryo-preserved cells or tissue sections as described (Braig et al., 2005; Dimri et al., 1995). Cases were considered senescent if their mean percentage of SA-β-gal-positive cells was higher than the mean percentage of Ki67-positive cells.

Ras **mutation analysis**

Genomic DNA was extracted from macro-dissected tumour ~~cell-enriched~~ areas of FFPE tissue sections using the QIAamp DNA Mini kit (Qiagen, Hilden, Germany). PCR amplification of the first exon of the *k-ras* gene was performed according to van den Brandt and colleagues (Brink et al., 2003). The resulting 179 bp PCR product was sequenced using the BigDye Terminator v1.1 Cycle Sequencing kit on a 3130 Genetic Analyzer (Applied Biosystems, Foster City, CA, USA). Hotspot codon 12 or 13 mutations were detected by comparison with the germ-line sequence.

Statistical analysis

Statistical analyses (SPSS software package, release 17.0, SPSS, Munich, Germany) of Kaplan-Meier survival plots were based on the log-rank (Mantel-Cox) test; additional statistical comparisons utilized the Wilcoxon-Mann-Whitney test (to probe equal distribution of age, frequency of Ki67-reactive and cleaved caspase 3-positive cells, and serum CEA levels in patient subgroups), the exact Fisher's test (with respect to gender, tumour localization, sites of distant metastasis [one *vs.* more than one], and *Ras* mutations), and the chi-square test (regarding the pT and the pN status). *P*-values < 0.05 were considered significant.

RESULTS

We analyzed 23 snap-frozen colorectal tissue samples of normal mucosa, adenomas, and untreated invasive carcinomas by the SA-β-gal assay, complemented by immunostaining for the proliferation marker Ki67, and confirmed the reportedly high frequency of senescent cells in adenomas, leading to the classification of 8 out of 12 adenoma cases tested as senescent, which is well in line with their macroscopic presentation as polyps of often stable size for years (Figure 1A and B; see the flow diagram in Figure 2A for technical details) (Bartkova et al., 2006). Importantly, as previously reported for a subset of lymphoma, lung and breast cancer specimens at manifestation (Reimann et al., 2010; Roberson et al., 2005; te Poele et al., 2002), we detected a significant fraction of senescent cells within neoplastic epithelial areas of manifest colorectal carcinomas, possibly indicating a still available senescence program at this full-blown cancer stage (Figure 1A and B).

Since the enzymatic SA-β-gal assay cannot be applied to FFPE routine samples, or substituted by a single marker, we tested protein expression levels of a panel of DDR mediators, cell-cycle regulators, chromatin-related proteins and others (Bartkova et al., 2006; Collado & Serrano, 2006) in a well-established OIS reference model system – sections of either snap-frozen or FFPE pellets of Ras-senescent *vs.* proliferating fibroblasts – that allowed us to compare SA-β-gal staining and potential immunohistochemical surrogate markers in the same material side by side (Serrano et al., 1997). Using this fibroblast model system followed by first a learning and then a validation set of adenoma samples, we generated a senescence surrogate score (senescence index, SI) based on the expression of p-ERK, HP1γ, and PAI-1 – all of them previously linked to OIS (Lin et al., 1998; Narita et al., 2003; Serrano et al., 1997)– that recapitulated SA-β-gal reactivity and adenoma senescence (Figure 1C, and Figure 2).

We obtained the SI in low-proliferating areas of 30 independent UICC stage IV colorectal cancer (CRC) samples prior to any drug treatment, and assigned these cases, based on a cut-off value, to a (partly) senescent *vs.* a non-senescent group. All patients in this retrospective analysis received a 5-FU/LV-based first-line regimen. Patients with senescent areas in their tumour biopsies experienced a significantly longer progression-free survival (PFS) with a median PFS of 12.0 *vs.* 6.0 months when compared to the non-senescent group (Figure 1D). Notably, both groups did not exhibit statistically significant differences with respect to gender, age, pT and pN status as well as localization of the primary tumour (colon *vs.* rectum), extent of distant metastasis (one *vs.* more than one site), or CEA serum levels at diagnosis, and exhibited indistinguishable rates of proliferation (*i.e.* averaged sample-wide Ki67 reactivity) and apoptosis (*i.e.* mean frequency of cleaved caspase 3-positive cells) (data not shown). Interestingly, K-*Ras* codon 12/13 mutations were found at a higher frequency (*P* = 0.035) in the senescent group (Figure 1D; insert), suggesting that *Ras* mutations, if associated with a senescent phenotype, may not necessarily serve as a predictor of poor outcome, as reported by several studies in the past (Andreyev et al., 2001; Andreyev et al., 1998; Benhattar et al., 1993; Roth et al., 2010).

DISCUSSION

This is the first report linking cellular senescence at diagnosis to treatment outcome in cancer. Whether sporadic senescent cells in manifest tumours represent a few remainders of the pre-

malignant condition, or indicate retained senescence susceptibility throughout the tumour is currently not clear. Our data favour the latter explanation, postulating that TIS produced in response to DNA-damaging chemotherapy in senescence-capable tumour cells contributes to the overall outcome to therapy. Notably, an inverse correlation between the expression level of another senescence marker, macroH2A, and the risk of recurrence has recently been reported for lung cancer patients (Sporn et al., 2009; Zhang et al., 2005). Additional studies are certainly needed to clarify whether a greater extent of sporadic cancer cell senescence indeed translates into a higher frequency of TIS-positive cells *in situ* when analyzed in re-biopsies a few days after chemotherapy. Moreover, a preserved pro-senescent cancer capability might be therapeutically exploitable by novel senescence-inducing strategies that do no longer damage DNA. The role of senescent cells at diagnosis as a novel predictor of treatment outcome should be further evaluated in larger prospective trials.

ACKNOWLEDGEMENTS

REFERENCES

Andreyev, H.J., Norman, A.R., Cunningham, D., Oates, J., Dix, B.R., Iacopetta, B.J., Young, J., Walsh, T., Ward, R., Hawkins, N., Beranek, M., Jandik, P., Benamouzig, R., Jullian, E., Laurent-Puig, P., Olschwang, S., Muller, O., Hoffmann, I., Rabes, H.M., Zietz, C., Troungos, C., Valavanis, C., Yuen, S.T., Ho, J.W., Croke, C.T., O'Donoghue, D.P., Giaretti, W., Rapallo, A., Russo, A., Bazan, V., Tanaka, M., Omura, K., Azuma, T., Ohkusa, T., Fujimori, T., Ono, Y., Pauly, M., Faber, C., Glaesener, R., de Goeij, A.F., Arends, J.W., Andersen, S.N., Lovig, T., Breivik, J., Gaudernack, G., Clausen, O.P., De Angelis, P.D., Meling, G.I., Rognum, T.O., Smith, R., Goh, H.S., Font, A., Rosell, R., Sun, X.F., Zhang, H., Benhattar, J., Losi, L., Lee, J.Q., Wang, S.T., Clarke, P.A., Bell, S., Quirke, P., Bubb, V.J., Piris, J., Cruickshank, N.R., Morton, D., Fox, J.C., Al-Mulla, F., Lees, N., Hall, C.N., Snary, D., Wilkinson, K., Dillon, D., Costa, J., Pricolo, V.E., Finkelstein, S.D., Thebo, J.S., Senagore, A.J., Halter, S.A., Wadler, S., Malik, S., Krtolica, K. & Urosevic, N. (2001). Kirsten ras mutations in patients with colorectal cancer: the 'RASCAL II' study. *Br J Cancer*, **85,** 692-6.

Andreyev, H.J., Norman, A.R., Cunningham, D., Oates, J.R. & Clarke, P.A. (1998). Kirsten ras mutations in patients with colorectal cancer: the multicenter "RASCAL" study. *J Natl Cancer Inst*, **90,** 675-84.

Bartkova, J., Horejsi, Z., Koed, K., Kramer, A., Tort, F., Zieger, K., Guldberg, P., Sehested, M., Nesland, J.M., Lukas, C., Orntoft, T., Lukas, J. & Bartek, J. (2005). DNA damage response as a candidate anti-cancer barrier in early human tumorigenesis. *Nature*, **434,** 864-70.

Bartkova, J., Rezaei, N., Liontos, M., Karakaidos, P., Kletsas, D., Issaeva, N., Vassiliou, L.V., Kolettas, E., Niforou, K., Zoumpourlis, V.C., Takaoka, M., Nakagawa, H., Tort, F., Fugger, K., Johansson, F., Sehested, M., Andersen, C.L., Dyrskjot, L., Orntoft, T., Lukas, J., Kittas, C., Helleday, T., Halazonetis, T.D., Bartek, J. & Gorgoulis, V.G. (2006). Oncogene-induced senescence is part of the tumorigenesis barrier imposed by DNA damage checkpoints. *Nature*, **444,** 633-7.

Benhattar, J., Losi, L., Chaubert, P., Givel, J.C. & Costa, J. (1993). Prognostic significance of K-ras mutations in colorectal carcinoma. *Gastroenterology*, **104,** 1044-8.

Braig, M., Lee, S., Loddenkemper, C., Rudolph, C., Peters, A.H., Schlegelberger, B., Stein, H., Dorken, B., Jenuwein, T. & Schmitt, C.A. (2005). Oncogene-induced senescence as an initial barrier in lymphoma development. *Nature*, **436,** 660-5.

Brink, M., de Goeij, A.F., Weijenberg, M.P., Roemen, G.M., Lentjes, M.H., Pachen, M.M., Smits, K.M., de Bruine, A.P., Goldbohm, R.A. & van den Brandt, P.A. (2003). K-ras oncogene mutations in sporadic colorectal cancer in The Netherlands Cohort Study. *Carcinogenesis*, **24,** 703-10.

Brown, J.M. & Attardi, L.D. (2005). The role of apoptosis in cancer development and treatment response. *Nat Rev Cancer*, **5,** 231-7.

Chang, B.D., Broude, E.V., Dokmanovic, M., Zhu, H., Ruth, A., Xuan, Y., Kandel, E.S., Lausch, E., Christov, K. & Roninson, I.B. (1999). A senescence-like phenotype distinguishes tumor cells that undergo terminal proliferation arrest after exposure to anticancer agents. *Cancer Res*, **59,** 3761-7.

Collado, M. & Serrano, M. (2006). The power and the promise of oncogene-induced senescence markers. *Nat Rev Cancer*, **6,** 472-6.

Collado, M. & Serrano, M. (2010). Senescence in tumours: evidence from mice and humans. *Nat Rev Cancer*, **10,** 51-7.

Dimri, G.P., Lee, X., Basile, G., Acosta, M., Scott, G., Roskelley, C., Medrano, E.E., Linskens, M., Rubelj, I., Pereira-Smith, O. & et al. (1995). A biomarker that identifies senescent human cells in culture and in aging skin in vivo. *Proc Natl Acad Sci U S A*, **92,** 9363-7.

Gorgoulis, V.G., Vassiliou, L.V., Karakaidos, P., Zacharatos, P., Kotsinas, A., Liloglou, T., Venere, M., Ditullio, R.A., Jr., Kastrinakis, N.G., Levy, B., Kletsas, D., Yoneta, A., Herlyn, M., Kittas, C. & Halazonetis, T.D. (2005). Activation of the DNA damage checkpoint and genomic instability in human precancerous lesions. *Nature*, **434,** 907-13.

Lin, A.W., Barradas, M., Stone, J.C., van Aelst, L., Serrano, M. & Lowe, S.W. (1998). Premature senescence involving p53 and p16 is activated in response to constitutive MEK/MAPK mitogenic signaling. *Genes Dev*, **12,** 3008-19.

Michaloglou, C., Vredeveld, L.C., Soengas, M.S., Denoyelle, C., Kuilman, T., van der Horst, C.M., Majoor, D.M., Shay, J.W., Mooi, W.J. & Peeper, D.S. (2005). BRAFE600-associated senescence-like cell cycle arrest of human naevi. *Nature*, **436,** 720-4.

Narita, M., Nunez, S., Heard, E., Lin, A.W., Hearn, S.A., Spector, D.L., Hannon, G.J. & Lowe, S.W. (2003). Rb-mediated heterochromatin formation and silencing of E2F target genes during cellular senescence. *Cell*, **113,** 703-16.

Reimann, M., Lee, S., Loddenkemper, C., Dörr, J.R., Tabor, V., Aichele, P., Stein, H., Dörken, B., Jenuwein, T. & Schmitt, C.A. (2010). Tumor stroma-derived TGF-ß limits Myc-driven lymphomagenesis via Suv39h1-dependent senescence. *Cancer Cell*, **17,** 262-72.

Roberson, R.S., Kussick, S.J., Vallieres, E., Chen, S.Y. & Wu, D.Y. (2005). Escape from therapy-induced accelerated cellular senescence in p53-null lung cancer cells and in human lung cancers. *Cancer Res*, **65,** 2795-803.

Roth, A.D., Tejpar, S., Delorenzi, M., Yan, P., Fiocca, R., Klingbiel, D., Dietrich, D., Biesmans, B., Bodoky, G., Barone, C., Aranda, E., Nordlinger, B., Cisar, L., Labianca, R., Cunningham, D., Van Cutsem, E. & Bosman, F. (2010). Prognostic role of KRAS and BRAF in stage II and III resected colon cancer: results of the translational study on the PETACC-3, EORTC 40993, SAKK 60-00 trial. *J Clin Oncol*, **28,** 466-74.

Schmitt, C.A. (2003). Senescence, apoptosis and therapy - cutting the lifelines of cancer. *Nat Rev Cancer*, **3,** 286-95.

Schmitt, C.A. (2007). Cellular senescence and cancer treatment. *Biochim Biophys Acta*, **1775,** 5-20.

Schmitt, C.A., Fridman, J.S., Yang, M., Lee, S., Baranov, E., Hoffman, R.M. & Lowe, S.W. (2002). A senescence program controlled by p53 and p16INK4a contributes to the outcome of cancer therapy. *Cell*, **109,** 335-46.

Serrano, M., Lin, A.W., McCurrach, M.E., Beach, D. & Lowe, S.W. (1997). Oncogenic ras provokes premature cell senescence associated with accumulation of p53 and p16INK4a. *Cell*, **88,** 593-602.

Sporn, J.C., Kustatscher, G., Hothorn, T., Collado, M., Serrano, M., Muley, T., Schnabel, P. & Ladurner, A.G. (2009). Histone macroH2A isoforms predict the risk of lung cancer recurrence. *Oncogene*, **28,** 3423-8.

te Poele, R.H., Okorokov, A.L., Jardine, L., Cummings, J. & Joel, S.P. (2002). DNA damage is able to induce senescence in tumor cells in vitro and in vivo. *Cancer Res*, **62,** 1876-83.

Yerushalmi, R., Woods, R., Ravdin, P.M., Hayes, M.M. & Gelmon, K.A. (2010). Ki67 in breast cancer: prognostic and predictive potential. *Lancet Oncol*, **11,** 174-83.

Zhang, R., Poustovoitov, M.V., Ye, X., Santos, H.A., Chen, W., Daganzo, S.M., Erzberger, J.P., Serebriiskii, I.G., Canutescu, A.A., Dunbrack, R.L., Pehrson, J.R., Berger, J.M., Kaufman, P.D. & Adams, P.D. (2005). Formation of MacroH2A-containing senescence-associated heterochromatin foci and senescence driven by ASF1a and HIRA. *Dev Cell*, **8,** 19-30.

Figure Legends

Figure 1 Stratification of stage IV CRC samples by a senescence index (SI) predicts PFS to first-line 5-FU/LV therapy. (**A**) Proportions of senescent cases in cryo-preserved colorectal tissue sections of the indicated groups (normal crypt mucosa [n = 5 (0 senescent)]; adenoma [n = 12 (8 senescent)], invasive carcinoma [n = 6 (1 senescent)]). Note that 9/12 adenoma and 2/6 carcinoma cases would score "senescent" if judged in low-proliferating areas only (see **D**). (**B**) Average frequency of senescent cells per group (as in **A**), measured as the percentage of SA-β-gal-positive (blue) cells, and compared to the rate of Ki67-positive (red nuclear staining) cells (*top:* error bars represent the standard deviation; *bottom:* matched areas of representative photomicrographs – a non-senescent normal crypt mucosa, a senescent adenoma, and a formally non-senescent carcinoma [but displaying numerous senescent cells]). Notably, in normal colorectal mucosa, only cells of the most differentiated luminal mucosa stain SA-β-gal-positive. (**C**) FFPE sections of pelleted Ras-infected senescent (sen.) human fibroblasts (SA-β-gal-positive and Ki67-negative frozen material as a reference) exhibit much stronger immunoreactivity for p-ERK, HP1γ, and cytoplasmic PAI-1 when compared to non-senescent (non-sen.) mock-infected fibroblasts. (**D**) SI values, based on the expression of these three markers, were obtained in 30 cases of stage IV CRC specimens at diagnosis, and utilized to stratify PFS following 5-FU/LV first-line chemotherapy (senescent [n = 12; blue line] *vs.* non-senescent [n = 17; red line]; one case scored "not conclusive" [see Figure 2B]). Genomic sequencing in a subset of these 29 specimens identified K-*Ras* codon 12 or 13 mutations in 5/6 senescent, but only 2/11 non-senescent cases (*insert*). Note that a primary stratification by the K-*Ras* mutation status unveiled no significant differences in PFS (P = 0.128).

Figure 2 Generation and validation of the senescence index (SI). (**A**) Technical flow diagram of the generation and application of the senescence index (SI) in a *Ras*-transduced human fibroblast cell line and in colorectal tissue specimens. (**B**) Formula and cut-off values of the SI based on the expression p-ERK, HP1γ and PAI-1. Coefficients reflect the reciprocal average percentage of cells that stained positive for the respective marker in the learning adenomas to normalize the relative weight of the three markers. The correction value −19 was chosen to set the discrimination threshold at 0, with the range between −1 and +1 considered "non-conclusive". (**C**) The majority of validation set adenomas is senescent when analyzed by the SI. A set of 7 matched samples (frozen and FFPE material from the same adenoma) underscores the high concordance between the SA-β-gal/Ki67- (see definition in "Materials and Methods") and the SI-based assignment.
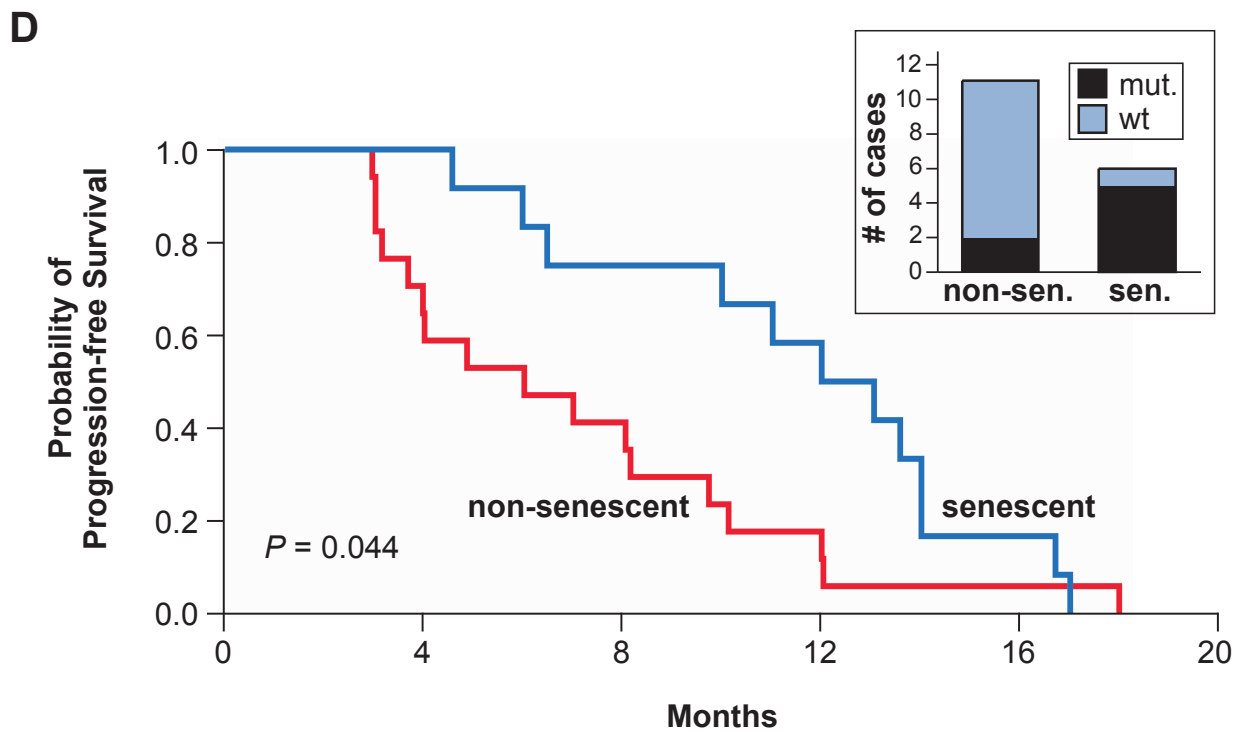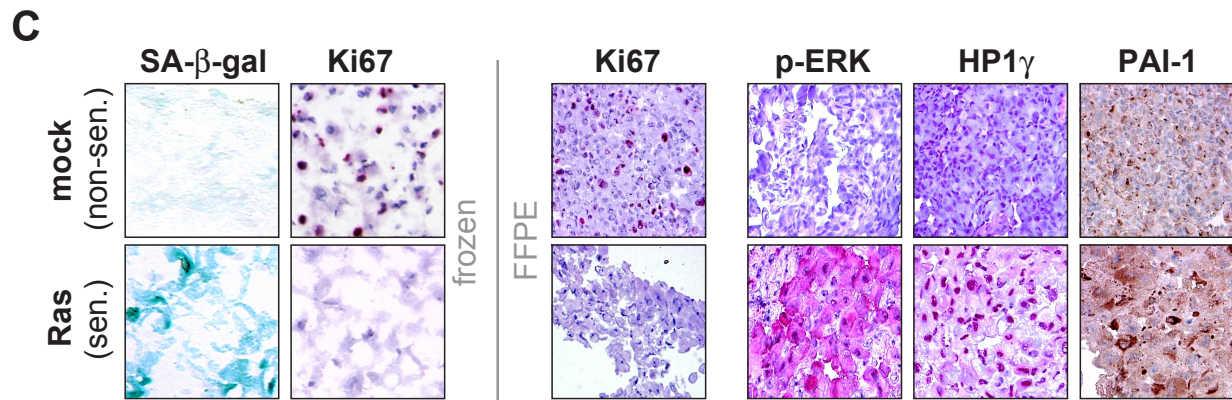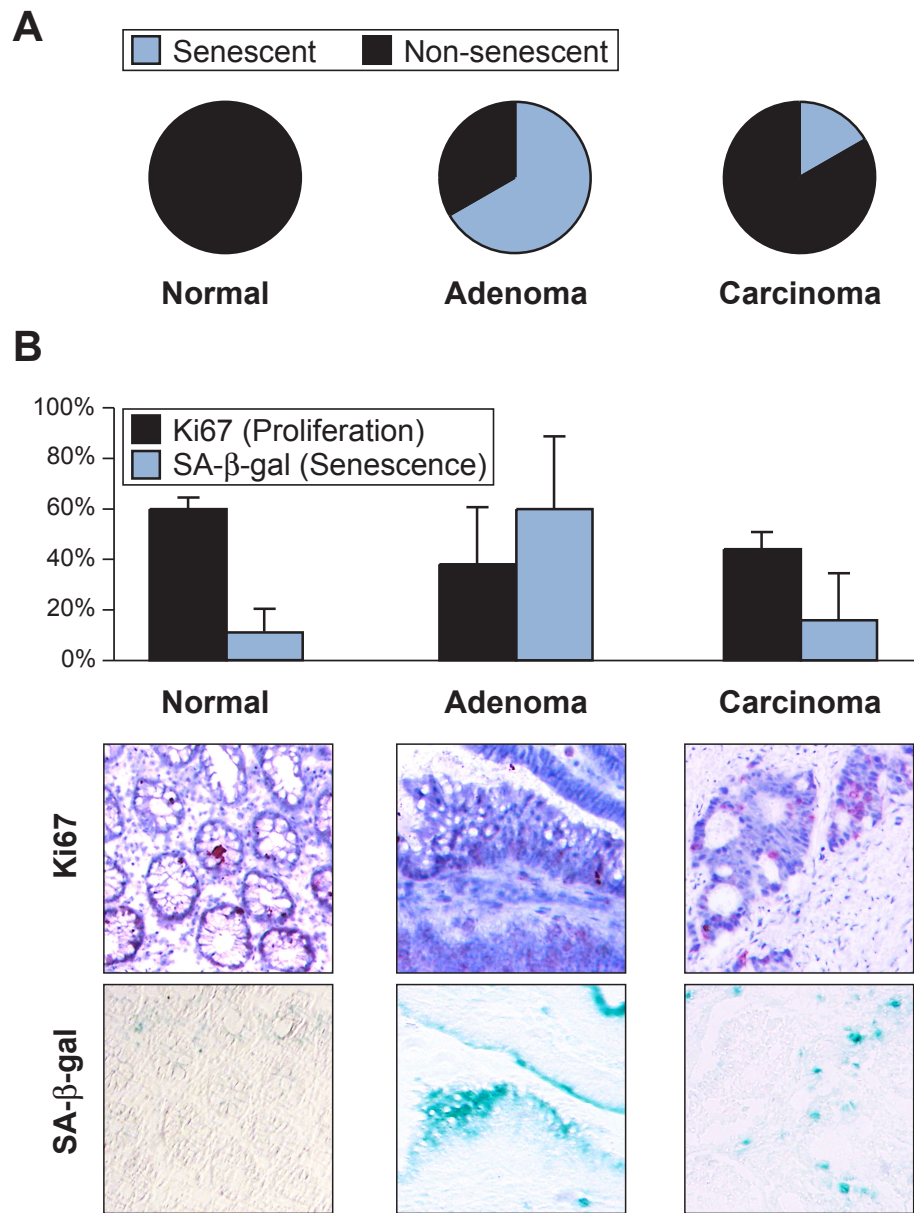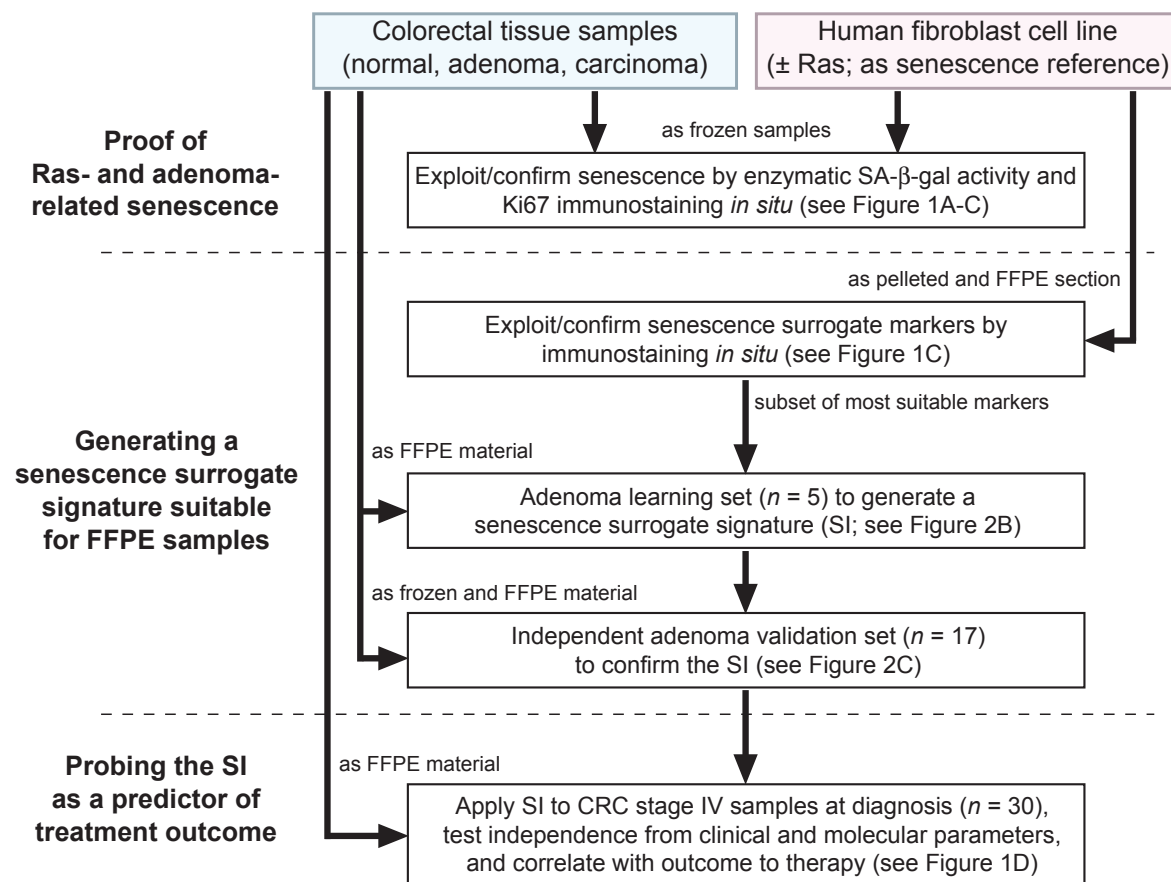
Figure 1 (Haugstetter et al.)

Figure 2 (Haugstetter et al.)

A

Senescence Index (SI)

Flow Diagram

B

$$SI = 34.5 \cdot p\text{-}ERK + 13.9 \cdot HP1\gamma + 11.4 \cdot PAI\text{-}1 - 19$$

(enter % positive cells as values from 0 to 1)

SI > +1: senescent
SI < -1: non-senescent
-1 ≤ SI ≥ +1: not conclusive

C

17 validation set adenomas analyzed by the SI:
- **11 senescent**
- **6 non-senescent**

7 matched frozen/FFPE validation set adenomas:

	Cryo	FFPE
Adenoma	**SA-β-gal/Ki67**	**SI**
#13	non-senescent	non-senescent
#14	non-senescent	non-senescent
#18	non-senescent	non-senescent
#15	senescent	senescent
#16	senescent	senescent
#17	senescent	senescent
#19	senescent	non-senescent